TEMPLATE FOR THE LOW-x MEETING 2011 PROCEEDINGS PREPARED BY LATEX *

H.S. LOWX2011-SPEAKER and B. LOWX2011-CO-AUTHOR

for the Compostela Collaboration

Dpto. Física de Partículas and
Instituto galego de Física de Altas Enerxías
Universidade de Santiago de Compostela
Santiago de Compostela 15782
Galice, Spain
E-mail: name.author@Lowx2011.org

This is abstract for your Low-x 2011 Meeting contribution. It should be a few lines briefly describing your contribution to the Proceedings. Please, remember that deadline for your contribution is November 15^{th}, 2011.

1 Guidelines

Please, find attached a Latex class file: $'Lowx2011.cls'$ for preparation of your Low-x Meeting 2011 contribution. We recommend all speakers also to use this Latex-file $'Lowx2011\_temp.tex'$ with EPS-figure $'Lowx2011Fig.ps'$ as a template for their Proceedings contributions.

2 Limits of Low-x Meeting 2011 contributions

The limit for the size of a Low-x Meeting 2011 contribution:
8 pages for (20+5 and more minutes) talks and up to 6 pages for discussion sessions.

*This work is supported by the High-Energy Physics Foundation

3 Where to send your contribution

Please, send your contribution by e-mail:
merino@fpaxp1.usc.es and *royon@hep.saclay.cea.fr*
with subject: speaker name

4 Deadline for your contribution to the Low-x Meeting 2011 Proceedings

October 31^st, 2011

5 Figures

Please prepare the figures in high resolution (300 dpi) for half-tone pictures. Half-tone pictures must be sharp enough for reproduction, otherwise they will be rejected.

6 Text sample

The Quark-Gluon String Model (QGSM) and the Dual Parton Model (DPM) are based on the Dual Topological Unitarization (DTU) and they describe quite reasonably many features of high energy production processes in both hadron-nucleon and hadron-nucleus collisions [1, 2, 3, 4, 5]. High energy interactions are considered as taking place via the exchange of one or several Pomerons, all elastic and inelastic processes resulting from cutting through or between Pomerons [6]. Inclusive spectra of hadrons are related to the corresponding fragmentation functions of quarks and diquarks, which are constructed using the Reggeon counting rules [7].

In the string models, baryons are considered as configurations consisting of three connected strings (related to three valence quarks) called string junction (SJ) [8, 9, 10]. In the processes of secondary production the SJ diffusion in rapidity space leads to significant differences in the yields of baryons and antibaryons in the midrapidity region even at very high energies [11].

On the other hand, in QCD, the hadrons are composite bound state configurations built up from the N_c quark, and $N_c^2 - 1$ gluon fields. In the string models the colour part of a baryon wave function can be defined as a star (or Y) configuration [8, 10] that is supported by lattice calculations.

This picture leads to some general phenomenological predictions. In particular, the baryon number transfer to large rapidity distances in hadron-nucleon and hadron-nucleus inclusive reactions can be explained by SJ diffusion.

To perform more quantitative predictions a model for multiparticle production has to be adopted. In the present paper we have used the QGSM for the numerical calculations.

For a nucleon target, the inclusive spectrum of a secondary hadron h has the form [1]:

$$\frac{dn}{dy} \;=\; \frac{x_E}{\sigma_{inel}}\frac{d\sigma}{dx_F} \;=\; \sum_{n=1}^{\infty} w_n \phi_n^h(x) \;, \tag{1}$$

where the functions $\phi_n^h(x)$ determine the contribution of diagrams with n cut Pomerons and w_n is the relative weight of this diagram.

For pp collisions

$$\begin{aligned} \phi_{pp}^h(x) \;&=\; f_{qq}^h(x_+,n) f_q^h(x_-,n) + f_q^h(x_+,n) f_{qq}^h(x_-,n) \\ &\qquad + 2(n-1) f_s^h(x_+,n) f_s^h(x_-,n) \;, \end{aligned} \tag{2}$$

where f_{qq}, f_q, and f_s correspond to the contributions of diquarks, valence quarks, and sea quarks, respectively.

These functions are determined by the convolution of the diquark and quark distributions with the fragmentation functions. Both the diquark and quark distributions, which are normalized to unity, and the fragmentation functions are determined by Regge intercepts [7].

At very high energies both x_+ and x_- are negligibly small in the midrapidity region. In this case all fragmentation functions, which are usually written [7] as $G_q^h(z) = a_h(1-z)^\beta$, are constants, what leads to

$$\frac{dn}{dy} \;=\; g_h \cdot (s/s_0)^{\alpha_P(0)-1} \sim a_h^2 \cdot (s/s_0)^{\alpha_P(0)-1} \;, \tag{3}$$

expression which corresponds to the only one-Pomeron exchange diagram in Fig. 1a, that is, to the only diagram contributing to the inclusive density in the central region (AGK theorem [6]). The intercept of the supercritical Pomeron $\alpha_P(0) = 1 + \Delta$, $\Delta = 0.139$ [5], is used in the numerical calculations.

According to [12], we consider three different possibilities to obtain the net baryon charge. The first one is the fragmentation of the diquark giving rise to a leading baryon (Fig. 2a). A second possibility is to produce a leading meson in the first break-up of the string and a baryon in the subsequent break-up [7] (Fig. 2b). In these two cases the baryon number transfer is possible only for short distances in rapidity. In the third case,

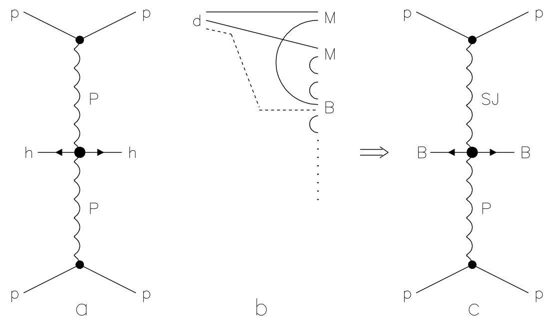

Figure 1: (a) One-Pomeron-pole diagram determining secondary hadron h production. (b) String Junction (shown by dashed line) diffusion leading to asymmetry in baryon/antibaryon production in the central region, and (c) the Reggeon diagram with String Junction exchange which describes the process shown in (b).

shown in Fig. 2c, both initial valence quarks recombine with sea antiquarks into mesons M and a secondary baryon is formed by the SJ together with three sea quarks.

The expressions of the corresponding fragmentation functions for the secondary baryon B production through the processes shown in Figs. 2a, 2b, and 2c (see [12]) can be found by simple quark combinatorics. The fraction z of the incident baryon energy carried by the secondary baryon decreases from Fig. 2a to Fig. 2c, whereas the mean rapidity gap between the incident and secondary baryon increases. The first two processes can not contribute to the inclusive spectra in the central region, but the third contribution is essential if the value of the intercept of the SJ exchange Regge-trajectory, α_{SJ}, is close to unity. The contribution of the graph in Fig. 2c has a coefficient ε which determines the small probability of such baryon number transfer.

In [12] the value $\alpha_{SJ} = 0.5$ was used. However, for such value of α_{SJ} different values of ε were needed for the correct

description of the experimental data at moderate and high energies. This problem was solved in [13], where it was shown with the help of more recent experimental data that all the data can be described with the parameter values

$$\alpha_{SJ} = 0.9 \quad \text{and} \quad \varepsilon = 0.024\,. \tag{4}$$

The probabilities w_n in Eq. (1) are calculated in the frame of Reggeon theory [1]. The normalization constants a_π (pion production), a_K (kaon production), $a_{\bar{N}}$ ($B\bar{B}$ pair

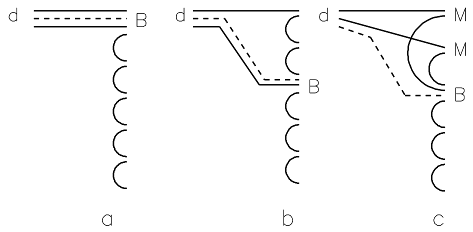

Figure 2: (a) QGSM diagrams describing secondary baryon B production by diquark d: initial SJ together with two valence quarks and one sea quark, (b) initial SJ together with one valence quark and two sea quarks, (c) and initial SJ together with three sea quarks.

production), and a_N (baryon production due to SJ diffusion) were determined [1, 2, 5] from the experimental data at fixed target energies, where the fragmentation functions are not constants. The values of these parameters have not been modified for the present calculations [14], while the values of correspondent constants for hyperons have been calculated by quark combinatorics. For sea quarks we have:

$$p : n : \Lambda + \Sigma : \Xi^0 : \Xi^- : \Omega = 4L^3 : 4L^3 : 12L^2S : 3LS^2 : 3LS^2 : S^3 \,. \tag{5}$$

The ratio S/L determines the strange suppression factor, and $2L+S = 1$. Usually in soft processes the ratio $\lambda = S/L$ is assumed to be 0.2−0.35. Inside this region it should be considered as a free parameter and in the numerical calculation we have used the value $\lambda = S/L = 0.25$ that leads to the best agreement with the data [15].

The calculated inclusive densities of different secondaries at RHIC, $\sqrt{s} = 200$ GeV, and LHC, $\sqrt{s} = 14$ TeV, energies [14] are presented in Table 1, where one can see that the agreement of the QGSM calculations with RHIC experimental data [15] is reasonably good.

The ratios of $\bar{p}/p$ production in pp interactions at $\sqrt{s} = 200$ GeV as the functions of rapidity have been calculated in the QGSM with the same parameters used in [16], and they are in reasonable agreement with the experimental data if the SJ contribution with $\varepsilon = 0.024$ is included, while the disagreement is evident for the calculation without SJ contribution (i.e. with $\varepsilon = 0$). One has to note that at asymptotically high energies the ratio $\bar{p}/p$ in the central region is expected to be equal to the unity, and so, some specific explanation is needed for any deviation from unity in this regime. One can see in Table 1 that at the RHIC energies the SJ contribution makes the deviation of $\bar{p}p$ from unity in the midrapidity region about three times bigger than in the calculation without SJ contribution.

Particle	RHIC ($\sqrt{s} = 200$ GeV)			LHC ($\sqrt{s} = 14$ TeV)	
	$\varepsilon = 0$	$\varepsilon = 0.024$	Experiment [15]	$\varepsilon = 0$	$\varepsilon = 0.024$
π^+	1.27			2.54	
π^-	1.25			2.54	
K^+	0.13		0.14 ± 0.01	0.25	
K^-	0.12		0.14 ± 0.01	0.25	
p	0.0755	0.0861		0.177	0.184
$\overline{p}$	0.0707			0.177	
Λ	0.0328	0.0381	0.0385 ± 0.0035	0.087	0.0906
$\overline{\Lambda}$	0.0304		0.0351 ± 0.0032	0.0867	
Ξ^-	0.00306	0.00359	0.0026 ± 0.0009	0.0108	0.0112
$\overline{\Xi^+}$	0.00298		0.0029 ± 0.001	0.0108	
Ω^-	0.00020	0.00025	*	0.000902	0.000934
$\overline{\Omega^+}$	0.00020		*	0.000902	

$^*dn/dy(\Omega^- + \overline{\Omega^+}) = 0.00034 \pm 0.00019$

Table 1: The QGSM results for midrapidity yields dn/dy ($|y| < 0.5$) for different secondaries at RHIC and LHC energies. The results for $\varepsilon = 0.024$ are presented only when different from the case $\varepsilon = 0$.

The QGSM predicts the deviation of $\bar{p}p$ ratios from unity due to SJ contribution on the level of 3−4% accuracy even at the LHC energy. Without SJ contribution these ratios are exactly equal to unity.

The QGSM calculations [13] predict practically equal values of $\bar{B}/B$ ratios in midrapidity region independently on baryon strangeness, what is qualitatively confirmed by the RHIC data on Au-Au collisions. In the case of $\Omega/\bar{\Omega}$ production in pp collisions we obtain a non-zero asymmetry (i.e. more Ω than $\bar{\Omega}$), that is necessarily absent in the naive quark model or in all recombination models, since both Ω and $\bar{\Omega}$ have no common valence quarks with the incident particles.

In Fig. 3 we reproduce the experimental data on ratios of yields of different secondaries [15] together with our calculations. Agreement is good except for only the point of the $\bar{p}/\pi^-$ ratio. From the comparison of our results with experimental data presented in

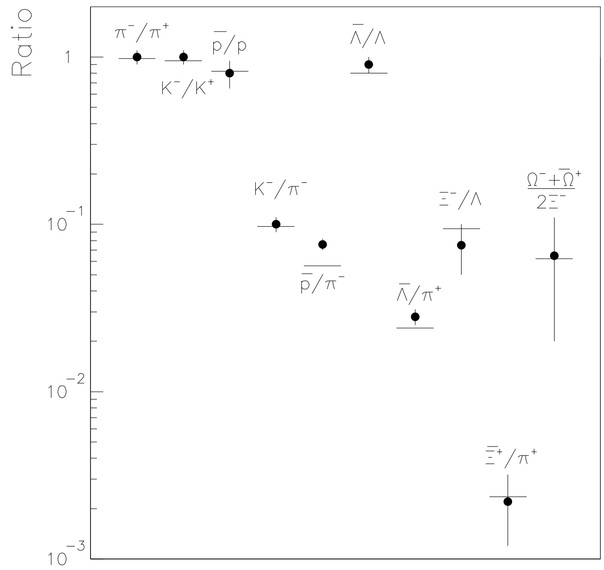

Figure 3: Ratios of different secondaries produced in midrapidity region in pp collisions at $\sqrt{s} = 200\,\text{GeV}$. Short horizontal solid lines show results of the QGSM calculations.

Table 1 and Fig. 3 we can conclude that the universal parameter $\lambda = 0.25$ describes the ratios of Λ/p, Ξ/Λ, and Ω/Ξ production in a reasonable way.

We discuss the role of string junction diffusion in the baryon charge transfer over large rapidity distances for the cases of pp collisions at RHIC and LHC energies. The inclusion of the SJ contribution provides a reasonable description of the main bulk of the existing experimental data. The calculations of the baryon/antibaryon yields and asymmetries without SJ contribution [12, 13] clearly diverge for most of the experimental data, where this contribution should be important.

Acknowledgements

We thank all Low-x Meeting 2011 participants for their contributions to the Low-x Meeting 2011 Proceedings. This work was supported in part by the High Energy Foundation and the World Science Agency.

Appendix

This is place for Appendix, if any.

References

[1] A.B. Kaidalov and K.A. Ter-Martirosyan, Yad. Fiz. **39**, 1545 (1984); **40**, 211 (1984).

[2] A.B. Kaidalov and O.I. Piskounova, Yad. Fiz. **41**, 1278 (1985); Z. Phys. **C30**,145 (1986).

[3] A. Capella, U. Sukhatme, C.I. Tan, and J. Tran Thanh Van, Phys. Rep. **236**, 225 (1994).

[4] A.B. Kaidalov, K.A. Ter-Martirosyan, and Yu.M. Shabelski, Yad. Fiz. **43**, 1282 (1986).

[5] Yu.M. Shabelski, Yad. Fiz. **44**, 186 (1986).

[6] V.A. Abramovsky, V.N. Gribov, and O.V. Kancheli, Yad. Fiz. **18**, 595 (1973).

[7] A.B. Kaidalov, Sov. J. Nucl. Phys. **45**, 902 (1987); Yad. Fiz. **43**, 1282 (1986).

[8] X. Artru, Nucl. Phys. B **85**, 442 (1975).

[9] M. Imachi, S. Otsuki, and F. Toyoda, Prog. Theor. Phys. **52**, 346 (1974); **54**, 280 (1976); **55**, 551 (1976).

[10] G.C. Rossi and G. Veneziano, Nucl. Phys. B **123**, 507 (1977).

[11] Yu.M. Shabelski, hep-ph/0211387.

[12] G.H. Arakelyan, A. Capella, A.B. Kaidalov and Yu.M. Shabelski, Eur. Phys. J. C **26**, 81 (2002); hep-ph/0103337.

[13] F. Bopp and Yu.M. Shabelski, Yad. Fiz. **68**, 2155 (2005); hep-ph/0406158.

[14] G.H. Arakelyan, C. Merino, and Yu.M. Shabelski, Yad. Fiz. **69**, 911 (2006); hep-ph/0505100; Phys. Atom. Nucl. **70**, 1110 (2007); hep-ph/0604103; Eur. Phys. J. **A31**, 519 (2007); hep-ph/0610264; hep-ph/0707.1491.

[15] B.I. Abelev *et al.*, STAR Collaboration, nucl-ex/0607033.

[16] F. Bopp and Yu.M. Shabelski, Eur. Phys. J. A **28**, 237 (2006); hep-ph/0603193.